Electrohydrodynamically Printed Flexible Organic Memristor for Leaky Integrate and Fire Neuron

Yichun Xu, Hongyang Wang, Dong Ye, Rui Yang, YongAn Huang, *Member, IEEE*, and Xiangshui Miao, *Senior Member, IEEE*

***Abstract*— Polymer memristors with good flexibility are promising electronic devices for edge computing paradigms in wearable electronics. However, most reported works present nonvolatile devices, which are suitable for applications in resistive random-access memory or artificial synapse. The volatile devices, which are indispensable in artificial neuron circuits, have rarely been reported, as the resistive switching property of organic devices is usually unstable in volatile devices. Moreover, most reported works use polymers in a way that is not compatible with traditional memristor fabrication technology, which limits the further applications of polymer memristors to large-scale neuromorphic circuits. In this letter, an Ag/Nafion/Au threshold switching memristor was fabricated via electrohydrodynamic printing technology and employed as a core of a leaky integrate and fire neuron circuit. The threshold switching memristor shows excel device size, good endurance, good device-to-device and cycle-to-cycle uniformity, flexibility, and stability at high temperatures. The combination of electrohydrodynamic printing technology and polymer memristor is promising in fast memristor production and largescale edge-computation network circuits.**

***Index Terms*— Artificial neuron, electrohydrodynamic printing, flexible electronics, polymer memristors, threshold switching.**

I. Introduction

MEMRISTIVE devices are creating evolutionary change in the emerging brain-inspired computing systems [1]–[6]. In particular, neuromorphic computing based on spiking neural networks (SNN) has attracted significant interest due to its low energy consumption and high similarity to biological neural systems [7], [8]. And threshold switching memristor (TSM) plays an important role in the oscillation neuron in neuromorphic circuits [9].

Flexible electronic devices offer many advantages over silicon, including thinness and deformability. Flexible electronics is of use in a wide range of applications including wearable sensors, e-skins, and microprocessors [10]–[14].

The integration of flexible memristors to fields like edge computing, which could effectively solve the real-time processing and energy consumption problems, is promising. And organic memristor is typically outstanding in this field as most polymers are inborn flexible. Though organic memristors have been researched widely [15]–[22], the reported devices mainly focus on nonvolatile properties. Little attention had been taken to volatile devices, which are important in building artificial neurons. Also, organic devices usually suffer from low endurance, non-compatibility with traditional fabrication technology, and high cost of experimental materials.

To solve these problems, this letter adopted the electrohydrodynamic (EHD) printing technology, which could fabricate continuous, smooth, and high-resolution electrodes in large-scale and fast production [23], [24]. The EHD printing is especially suitable for flexible devices. This letter also adopted Nafion, an off-the-shelf polymer, which is widely used as a proton exchange membrane and is relatively inexpensive. Nafion has parallel cylindrical nanochannels inside the membrane [25], which is reported that enable active metal cation to pass the membrane [26], [27]. These nanochannels facilitate metal to form filaments, like silver or copper filaments, which was reported in the previous work [26]. Based on these, a flexible, all-printed organic TSM was made, which reached stable resistive switching (RS) performance as well as good device-to-device and cycle-to-cycle uniformity. Then, based on the TSM, a leaky integrate and fire (LIF) neuron was made to show the potential application of the device.

II. Experiments

The device with an Ag/Nafion/Au cross-point structure, as shown in Fig.1(a), was fabricated on a PET substrate by an EHD Jet-H printer (Guangdong Sygole Intelligent Technology Co. Ltd.) in a continuous manner[24]. The EHD printing

Manuscript received October 28, 2021; accepted November 16, 2021. Date of publication November 18, 2021; date of current version December 29, 2021. This work was supported by the National Natural Science Foundation of China under Grant U1832116, Grant 51925503, and Grant 51772112. The review of this letter was arranged by Editor D. Kuzum. *(Yichun Xu and Hongyang Wang contributed equally to this work.) (Corresponding authors: Rui Yang; YongAn Huang.)*

Yichun Xu, Rui Yang, and Xiangshui Miao are with the Wuhan National Laboratory for Optoelectronics, School of Optical and Electronic Information, School of Integrated Circuits, Huazhong University of Science and Technology, Wuhan 430074, China, and also with Hubei Yangtze Memory Laboratories, Wuhan 430205, China (e-mail: yangrui@hust.edu.cn).

Hongyang Wang, Dong Ye, and YongAn Huang are with the State Key Laboratory of Digital Manufacturing Equipment and Technology, Flexible Electronics Research Center, Huazhong University of Science and Technology, Wuhan 430074, China (e-mail: yahuang@hust.edu.cn).

Color versions of one or more figures in this letter are available at https://doi.org/10.1109/LED.2021.3129202.

Digital Object Identifier 10.1109/LED.2021.3129202

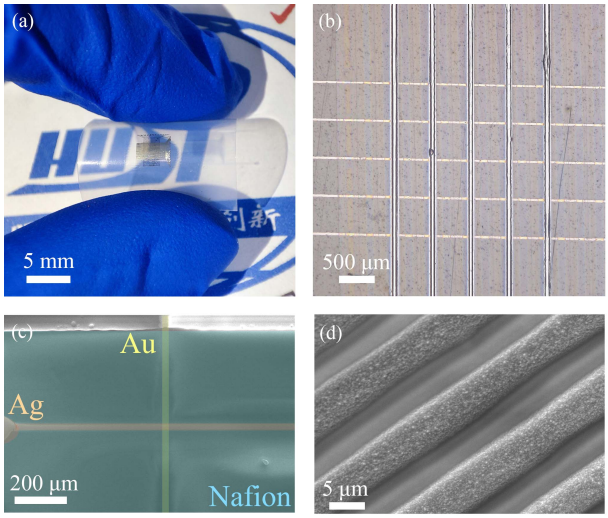

Fig. 1. (a) The overall view of printed 20 × 20 memristor array, (b) The optical microscopical photograph of the device, (c) The SEM photograph of Ag/Nafion/Au structure, and (d) The SEM photograph of Ag electrodes.

process is conducive to large-scale crossbar preparation, shown in Fig. 1(b). The size and thickness of the three layers were tuned by optimizing the printing parameters of the voltage, the nozzle height, the number of overprints, and so forth. The Ag and Au electrodes with the width of about 20 μm were obtained by glass nozzle with the diameter of 50 μm, and the uniform-thickness Nafion layer was obtained by metal nozzle with the diameter of 200 μm, as shown in Fig. 1(c). It should be mentioned that the width of printed Ag lines could reach about 6 μm (shown in Fig. 1(d)), which shows the possible smallest device size. The thickness of the three layers is 280 nm, 200 nm, 400 nm, respectively, measured by a Bruker Dimension Edge AFM. Then, the device was baked at 200 °C for 20 minutes to improve the conductivity of the Ag and Au electrode. The obtained wire resistances are about 40 Ω·cm for Ag and 130 Ω·cm for Au, respectively.

An Agilent B1500A semiconductor parameter analyzer was used to measure the device's electrical behaviors. A Tektronix AFG 31000 Arbitrary Function Generator was used to generate the voltage pulse and a Keysight DSOX3104T oscilloscope was used to capture the output waveforms. The simulation of LIF neurons was carried out in Python 3.9.6.

III. Results and Discussion

The typical threshold switching characteristic of the Ag/Nafion/Au devices is shown in Fig. 2(a), the device is forming-free. The distribution of threshold voltage (Vth) with a mean value of 1.5 V is shown in Fig. 2(b). It should be mentioned that the devices are from the same array. These results show the present organic TSM cell performs small cycle-to-cycle and device-to-device variations. It should also be mentioned that the yield of printed arrays is about 93%, which shows good uniformity of EHD printed devices. The volatile switching was also elucidated with pulse measurements (shown in Fig. 2(c)), during which fixed voltage pulses of 1.5V yielded incubation delay for about 250 μs and

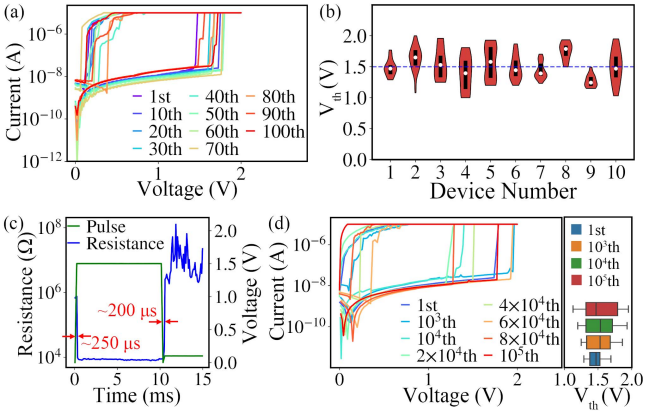

Fig. 2. (a) The I-V characteristic of Nafion TSM, (b) Device-to-device V_{th} distribution, (c) Pulse switching behavior of the Nafion TSM, and (d) I-V characteristic after pulse operation. The V_{th} distribution after different RS cycles is demonstrated in the right panel.

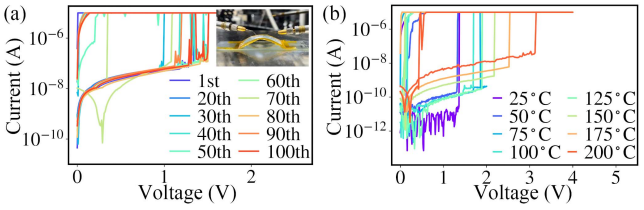

Fig. 3. (a) The I-V characteristic of Nafion TSM in bending circumstance, and (b) The I-V characteristic of Nafion TSM at different temperatures.

relaxation for about 200 μs. The endurance of the device after pulses are shown in Fig. 2(d), after 105 numbers of pulses, the device still shows stable RS abilities, indicating good endurance of the present device. As for the switching mechanism, there is a consensus that Ag filament formation/rupture dominates the switching process in most of the devices with Ag electrodes [6], [28]. Those formed Ag filaments are fragile under low compliance current in set process, which could break autonomously, thus the device exhibits volatile threshold switching property.

The mechanical flexibility of the TSM was measured, and experimental results were shown in Fig. 3(a). The bending angle is 20° of the PET substrate, with a curvature radius of 2.14 cm. No significant deterioration of RS properties is observed on the bending state, indicating good mechanical stability of the TSM. Organic devices are generally very vulnerable to high temperature [29], as most polymers degenerate under such situations. The high-temperature stability of Nafion enables the present device not to show a noticeable degeneration till the temperature is above 125°C, as shown in Fig. 3(b). As the temperature rises, the Vth and high resistance state (HRS) shows shifting to higher Vth and lower HRS, though the overall functions of the TSM are still operative at 200°C. The shifting of HRS and Vth might be related to the decrease of relative humidity and increase of the branch's crystallinity under high temperatures [30], which could hinder the formation of silver filaments.

The above experimental observations have indicated that the present Nafion TSM is endurable, uniform, flexible, and

TABLE I
COMPARISON WITH ORGANIC MEMRISTORS

Features	This work	[15]	[16]	[17]	[18]	[19]	[20]	[21]	[22]	[3]
Applications	Neuron	-	RRAM	RRAM	Synapse	Synapse	RRAM	RRAM	Memory	Logic
Endurance	$>10^5$	>50	-	>100	>300	$>10^4$	>50	>100	>500	>1000
Device size	6 μm	200 μm	100 μm	200 μm	200 μm	20 μm	-	200 μm	10 nm	100 nm
Flexibility	√	×	√	×	√	√	×	√	√	×
Fabrication method	All EHD printing	EHD Atomization +Screen printing	All EHD printing	Lithography	Lithography	Lithography	Lithography	Lithography	Lithography	Lithography
Cost	Low	Low	Medium	High	High	High	High	High	High	High
Working temperature	>200 °C	-	-	-	-	-	-	~150 °C	-	460 °C

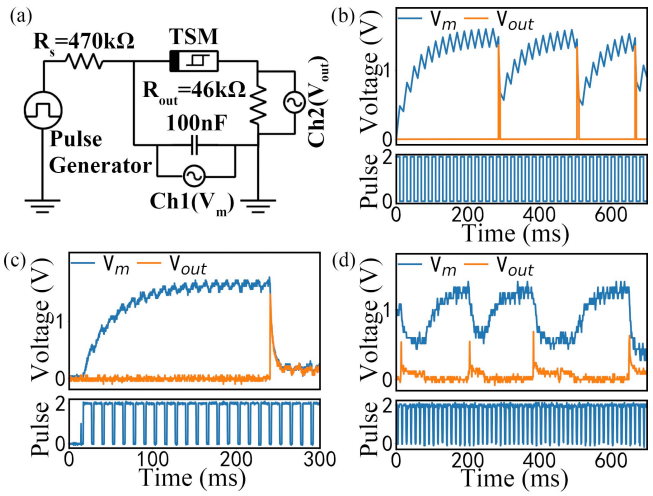

Fig. 4. (a) Schematic of the neuronal circuit built on a breadboard, (b) Simulation of the integrate and fire dynamics of the Nafion TSM based neuronal circuit, (c) Experimental measurement of one integrate and fire behavior, and (d) The continuous spike events of the Nafion TSM based neuronal circuit.

high-temperature stable, which shows the TSM is suitable to construct artificial neurons.

The LIF artificial neuron aims to replicate a neuron function related to the accumulation of electric charge through the cellular membrane. The TSM acts as a post-neuron to integrate the signals from inputs via a capacitor. When the accumulated capacitor potential approaches the V_{th}, the neuron fires and outputs a spiking pulse [31].

The circuit schematic of the TSM neuron with a connected synaptic resistor is shown in Fig. 4(a). The TSM device is in series with a resistor (R_{out} = 46 k), and the two components are in parallel with a capacitor (C = 100 nF). The neuron connects with a synapse resistor (R_s = 470 k). The input signal is a voltage pulse source applied to the left node. The change in the voltage on Rout is regarded as the output spike. Rout determines the compliance current for the TSM. Total amount of resistance in the HRS and in the LRS, Rout + RHRS and Rout + RLRS, respectively, defines the speed of charging and discharging in the respective loops during the spiking process. Therefore, Rout and Rs are carefully calculated by simulation to generate pulses in a proper response time and frequency.

The simulation result is shown in Fig. 4(b). An input voltage train with the pulse amplitudes of 2 V, widths 10 ms, and frequency 50 Hz is employed in the simulation. Wherein the RS parameters extracted from the IV curve of the Nafion TSM are implemented. The associated experimental parameters are all the same as the simulation except the frequency has changed to 80 Hz with 10 ms widths, the capacitor property of the TSM ascribed to this adjustment. The output voltage evolution Vout was demonstrated in Fig. 4(c) and (d). Fig. 4(c) shows the typical form of a spike, and Fig. 4(d) shows continuous spikes. These results show that the TSM neuron can successfully emulate the LIF function with a refractory period. It should be noted that this neuronal circuit is just a proof-of-concept experiment, while artificial neurons based on Nafion TSM devices don't require such large capacitance for a longer response time, which makes the detection easier. The neuronal circuit can work at a microsecond level as the switching speed of the device is at the range of ~0.2 ms (Fig.2(c)).

The comparison of the present device with other organic memristors is shown in Table I. As shown, the present device is unique in its application as an artificial neuron. The flexibility which is promising for wearable applications has also outweighed some organic devices based on silicon or glass. Comparing with other devices which also adopt EHD printing technology, the size of the present device is much smaller. It should be mentioned that the 6 μm device size is also very competitive compared with devices fabricated by lithography. The adopted commercial polymer has lowered the overall cost of the device, and as EHD printing is a kind of additive manufacturing technique, the whole fabrication procedure produces no wastes. Stability at high temperatures realized in the present device is rarely reported in other organic devices. Thus, the present flexible organic device performs impressive neural functions and potential in large-scale fabrication.

IV. CONCLUSION

In conclusion, a flexible TSM was experimentally demonstrated via EHD printing. The use of commercial polymer and EHD printing enables a fast, high-resolution, and economical memristor fabrication process. The TSM shows good endurance, device-to-device and cycle-to-cycle uniformity, and high-temperature stability. Based on the TSM, a LIF neuron was shown to welly emulate biological neuron function. The performance of the neuron unit has shown great potential in networks like the SNN. The combination of EHD printing and memristor has shown further applications in large-scale edge-computation crossbar arrays.

REFERENCES

[1] W. Zhang, B. Gao, J. Tang, P. Yao, S. Yu, M.-F. Chang, H.-J. Yoo, H. Qian, and H. Wu, "Neuro-inspired computing chips," *Nature Electron.*, vol. 3, no. 7, pp. 371–382, Jul. 2020, doi: 10.1038/s41928-020-0435-7.

[2] J. S. Najem, G. J. Taylor, R. J. Weiss, M. S. Hasan, G. Rose, C. D. Schuman, A. Belianinov, C. P. Collier, and S. A. Sarles, "Memristive ion channel-doped biomembranes as synaptic mimics," *ACS Nano*, vol. 12, no. 5, pp. 4702–4711, Mar. 2018, doi: 10.1021/acsnano.8b01282.

[3] B. Zhang, W. Chen, J. Zeng, F. Fan, J. Gu, X. Chen, L. Yan, G. Xie, S. Liu, Q. Yan, S. J. Baik, Z.-G. Zhang, W. Chen, J. Hou, M. E. El-Khouly, Z. Zhang, G. Liu, and Y. Chen, "90% yield production of polymer nano-memristor for in-memory computing," *Nature Commun.*, vol. 12, no. 1, Mar. 2021, Art. no. 1984, doi: 10.1038/s41467-021-22243-8.

[4] P. Yao, H. Wu, B. Gao, J. Tang, Q. Zhang, W. Zhang, J. J. Yang, and H. Qian, "Fully hardware-implemented memristor convolutional neural network," *Nature*, vol. 577, no. 7792, pp. 641–646, 2020, doi: 10.1038/s41586-020-1942-4.

[5] Q. Xia and J. J. Yang, "Memristive crossbar arrays for brain-inspired computing," *Nature Mater.*, vol. 18, no. 4, pp. 309–323, 2019, doi: 10.1038/s41563-019-0291-x.

[6] R. Yang, "Review of resistive switching mechanisms for memristive neuromorphic devices," *Chin. Phys. B*, vol. 29, no. 9, Sep. 2020, Art. no. 097305, doi: 10.1088/1674-1056/aba9c7.

[7] Q. Duan, Z. Jing, X. Zou, Y. Wang, K. Yang, T. Zhang, S. Wu, R. Huang, and Y. Yang, "Spiking neurons with spatiotemporal dynamics and gain modulation for monolithically integrated memristive neural networks," *Nature Commun.*, vol. 11, no. 1, p. 3399, Jul. 2020, doi: 10.1038/s41467-020-17215-3.

[8] R. Yang, H. Huang, and X. Guo, "Memristive synapses and neurons for bioinspired computing," *Adv. Electron. Mater.*, vol. 5, no. 9, Aug. 2019, Art. no. 1900287, doi: 10.1002/aelm.201900287.

[9] K. Wang, Q. Hu, B. Gao, Q. Lin, F.-W. Zhuge, D.-Y. Zhang, L. Wang, Y.-H. He, R. H. Scheicher, H. Tong, and X.-S. Miao, "Threshold switching memristor-based stochastic neurons for probabilistic computing," *Mater. Horizons*, vol. 8, no. 2, pp. 619–629, Feb. 2021, doi: 10.1039/D0MH01759K.

[10] Y. Wang, L. Yin, Y. Bai, S. Liu, L. Wang, Y. Zhou, C. Hou, Z. Yang, H. Wu, J. Ma, Y. Shen, P. Deng, S. Zhang, T. Duan, Z. Li, J. Ren, L. Xiao, Z. Yin, N. Lu, and Y. Huang, "Electrically compensated, tattoo-like electrodes for epidermal electrophysiology at scale," *Sci. Adv.*, vol. 6, no. 43, Oct. 2020, Art. no. eabd0996, doi: 10.1126/sciadv.abd0996.

[11] W. Gao, S. Emaminejad, H. Y. Y. Nyein, S. Challa, K. Chen, A. Peck, H. M. Fahad, H. Ota, H. Shiraki, D. Kiriya, D.-H. Lien, G. A. Brooks, R. W. Davis, and A. Javey, "Fully integrated wearable sensor arrays for multiplexed *in situ* perspiration analysis," *Nature*, vol. 529, pp. 509–514, Jan. 2016, doi: 10.1038/nature16521.

[12] Y. Huang, C. Zhu, W. Xiong, Y. Wang, Y. Jiang, L. Qiu, D. Guo, C. Hou, S. Jiang, Z. Yang, B. Wang, L. Wang, and Z. Yin, "Flexible smart sensing skin for 'fly-by-feel' morphing aircraft," *Sci. China Technol. Sci.*, 2021, doi: 10.1007/s11431-020-1793-0.

[13] Y. J. Park, B. K. Sharma, S. M. Shinde, M.-S. Kim, B. Jang, J.-H. Kim, and J.-H. Ahn, "All MoS_2-based large area, skin-attachable active-matrix tactile sensor," *ACS Nano*, vol. 13, no. 3, pp. 3023–3030, Mar. 2019, doi: 10.1021/acsnano.8b07995.

[14] S. Wang, J. Xu, W. Wang, G.-J. N. Wang, R. Rastak, F. Molina-Lopez, J. W. Chung, S. Niu, V. R. Feig, J. Lopez, T. Lei, S.-K. Kwon, Y. Kim, A. M. Foudeh, A. Ehrlich, A. Gasperini, Y. Yun, B. Murmann, J. B. H. Tok, and Z. Bao, "Skin electronics from scalable fabrication of an intrinsically stretchable transistor array," *Nature*, vol. 555, no. 7694, pp. 83–88, 2018, doi: 10.1038/nature25494.

[15] M. M. Rehman, B.-S. Yang, Y.-J. Yang, K. S. Karimov, and K. H. Choi, "Effect of device structure on the resistive switching characteristics of organic polymers fabricated through all printed technology," *Current Appl. Phys.*, vol. 17, no. 4, pp. 533–540, Apr. 2017, doi: 10.1016/j.cap.2017.01.023.

[16] S. Ali, J. Bae, C. H. Lee, S. Shin, and N. P. Kobayashi, "Ultra-low power non-volatile resistive crossbar memory based on pull up resistors," *Organic Electron.*, vol. 41, pp. 73–78, Feb. 2017, doi: 10.1016/j.orgel.2016.12.007.

[17] Q. Lin, S. Hao, W. Hu, M. Wang, Z. Zang, L. Zhu, J. Du, and X. Tang, "Human hair keratin for physically transient resistive switching memory devices," *J. Mater. Chem. C*, vol. 7, no. 11, pp. 3315–3321, Mar. 2019, doi: 10.1039/C8TC05334K.

[18] M.-K. Kim and J.-S. Lee, "Short-term plasticity and long-term potentiation in artificial biosynapses with diffusive dynamics," *ACS Nano*, vol. 12, no. 2, pp. 1680–1687, Jan. 2018, doi: 10.1021/acsnano.7b08331.

[19] Y. Choi, S. Oh, C. Qian, J.-H. Park, and J. H. Cho, "Vertical organic synapse expandable to 3D crossbar array," *Nature Commun.*, vol. 11, no. 1, pp. 1–9, Sep. 2020, doi: 10.1038/s41467-020-17850-w.

[20] J.-Q. Yang, L.-Y. Ting, R. Wang, J.-Y. Mao, Y. Ren, C.-L. Chang, C.-M. Yeh, H.-H. Chou, Y. Zhou, and S.-T. Han, "Fluorenone/carbazole based bipolar small molecules for non-volatile memory devices," *Organic Electron.*, vol. 78, Mar. 2020, Art. no. 105584, doi: 10.1016/j.orgel.2019.105584.

[21] Z. Lv, Q. Hu, Z. Xu, J. Wang, Z. Chen, Y. Wang, M. Chen, K. Zhou, Y. Zhou, and S. Han, "Organic memristor utilizing copper phthalocyanine nanowires with infrared response and cation regulating properties," *Adv. Electron. Mater.*, vol. 5, no. 4, Apr. 2019, Art. no. 1800793, doi: 10.1002/aelm.201800793.

[22] S. Goswami, A. J. Matula, S. P. Rath, S. Hedström, S. Saha, M. Annamalai, D. Sengupta, A. Patra, S. Ghosh, H. Jani, S. Sarkar, M. R. Motapothula, C. A. Nijhuis, J. Martin, S. Goswami, V. S. Batista, and T. Venkatesan, "Robust resistive memory devices using solution-processable metal-coordinated azo aromatics," *Nature Mater.*, vol. 16, pp. 1216–1224, Oct. 2017, doi: 10.1038/nmat5009.

[23] Q. Wang, G. Zhang, H. Zhang, Y. Duan, Z. Yin, and Y. Huang, "High-resolution, flexible, and full-color perovskite image photodetector via electrohydrodynamic printing of ionic-liquid-based ink," *Adv. Funct. Mater.*, vol. 31, no. 28, Apr. 2021, Art. no. 2100857, doi: 10.1002/adfm.202100857.

[24] M. S. Onses, E. Sutanto, P. M. Ferreira, A. G. Alleyne, and J. A. Rogers, "Mechanisms, capabilities, and applications of high-resolution electrohydrodynamic jet printing," *Small*, vol. 11, no. 34, pp. 4237–4266, Sep. 2015, doi: 10.1002/smll.201500593.

[25] K. Schmidt-Rohr and Q. Chen, "Parallel cylindrical water nanochannels in Nafion fuel-cell membranes," *Nature Mater.*, vol. 7, no. 1, pp. 75–83, Jan. 2008, doi: 10.1038/nmat2074.

[26] T. Tsuneda, "Fenton reaction mechanism generating no OH radicals in Nafion membrane decomposition," *Sci. Rep.*, vol. 10, no. 1, Oct. 2020, Art. no. 18144, doi: 10.1038/s41598-020-74646-0.

[27] M. P. Jayakrishnan, A. Vena, A. Meghit, B. Sorli, and E. Perret, "Nafion-based fully passive solid-state conductive bridging RF switch," *IEEE Microw. Wireless Compon. Lett.*, vol. 27, no. 12, pp. 1104–1106, Dec. 2017, doi: 10.1109/LMWC.2017.2764741.

[28] Y. van de Burgt, A. Melianas, S. T. Keene, G. Malliaras, and A. Salleo, "Organic electronics for neuromorphic computing," *Nature Electron.*, vol. 1, no. 7, pp. 386–397, Jul. 2018, doi: 10.1038/s41928-018-0103-3.

[29] X.-D. Huang, Y. Li, H.-Y. Li, K.-H. Xue, X. Wang, and X.-S. Miao, "Forming-free, fast, uniform, and high endurance resistive switching from cryogenic to high temperatures in $W/AlO_x/Al_2O_3/Pt$ bilayer memristor," *IEEE Electron Device Lett.*, vol. 41, no. 4, pp. 549–552, Apr. 2020, doi: 10.1109/LED.2020.2977397.

[30] B. R. Matos, M. A. Dresch, E. I. Santiago, L. P. R. Moraes, D. J. Carastan, J. Schoenmaker, I. A. Velasco-Davalos, A. Ruediger, A. C. Tavares, and F. C. Fonseca, "Nafion membranes annealed at high temperature and controlled humidity: Structure, conductivity, and fuel cell performance," *Electrochim. Acta*, vol. 196, pp. 110–117, Apr. 2016, doi: 10.1016/j.electacta.2016.02.125.

[31] X. Zhang, W. Wang, Q. Liu, X. Zhao, J. Wei, R. Cao, Z. Yao, X. Zhu, F. Zhang, H. Lv, S. Long, and M. Liu, "An artificial neuron based on a threshold switching memristor," *IEEE Electron Device Lett.*, vol. 39, no. 2, pp. 308–311, Feb. 2018, doi: 10.1109/LED.2017.2782752.